Imaging protein activity in live embryos using fluorescence resonance energy transfer biosensors

Elena Kardash, Jan Bandemer & Erez Raz

Institute for Cell Biology, Center for Molecular Biology of Inflammation, University of Münster, Münster, Germany. Correspondence should be addressed to E.R. (erez.raz@uni-muenster.de).

Published online 3 November 2011; doi:10.1038/nprot.2011.395

Fluorescence resonance energy transfer (FRET)-based molecular biosensors serve as important tools for studying protein activity in live cells and have been widely used for this purpose over the past decade. However, FRET biosensors are rarely used in the context of the live organism because of the inherent high cellular complexity and imaging challenges associated with the three-dimensional environment. Here we provide a protocol for using single-chain intramolecular FRET-based biosensors in early development. We provide a general protocol for FRET ratio imaging in embryos, including the data-acquisition conditions and the algorithm for ratio image generation. We then use the pRaichu RacFRET biosensor to exemplify the adaptation and optimization of a particular biosensor for use in live zebrafish embryos. Once an optimized biosensor is available, the complete procedure, including introduction of the probes into embryos, imaging and data analysis, requires 2–3 d.

INTRODUCTION

When investigating developmental and cell biological processes, it is important to determine the activation state of the relevant regulators. This is often performed by isolating the cells of interest and assaying the activation state of the protein biochemically. Such an approach is however of limited use when rapid processes that depend on specific context within the live tissue are concerned, or when the subcellular activation pattern is of interest. This requirement led to the development of alternative methods addressing this issue. To detect protein activation and function at subcellular resolutions in real time, genetically encoded biosensors have been developed. Such fluorescence-based sensors are used to convert molecular changes within the cell into an optical signal, which is then detected in an appropriate microscope setup[1]. The level of some signaling events can be evaluated by the accumulation of particular molecular products of protein activity in certain locations within the cell; alternatively, it can be evaluated by the absolute amount of the product. For example, activation of phosphoinositide 3-kinase results in the accumulation of the product phosphatidylinositol (3,4,5)-trisphosphate (PIP3) at the plasma membrane in parts of the cell where the enzyme is active[2,3]. PIP3 can be detected by biosensors consisting of fluorescent proteins fused to the pleckstrin homology (PH) domains of proteins that recognize and preferentially bind to PIP3. Such methods that rely on detecting the product of enzymes or the level of second messengers are indeed useful in some instances. In other cases, such as with Rho GTPases or kinase activity, measuring the activation state of the enzyme itself is more useful, as the active protein can act through different substrates and affect several pathways, some of which are unknown.

The activation of a molecule often manifests as a conformational change that alters the spatial positioning of protein domains or binding to other proteins. Such activation events can be detected using FRET. FRET is a process of the nonradiative energy transfer from a donor fluorophore to an acceptor fluorophore, both of which are placed in close proximity to one another[4,5]. By using the FRET phenomenon, biosensors—molecules that can report on various conditions in the cell—are often used for studying the spatial and temporal dynamics of protein activation in real time[6]. Although different types of such sensors have been generated[7] and both intermolecular (e.g., for Rac[8]) and intramolecular (e.g., for RhoA[9]) sensors have been developed, we focus here on the single-chain intramolecular FRET biosensors[6,10]. Biosensors of this class are made of a single molecule that typically consists of two protein functional domains (one termed 'sensor' and the other 'ligand') that can interact with one another and two fluorophores that act as donor or acceptor for the energy transfer (**Fig. 1a**). In response to a specific stimulus, the sensor interacts with the ligand, thereby altering the relative positioning of the donor and the acceptor proteins, which results in changes in the FRET efficiency (**Fig. 1**). The advantage of using single-chain FRET biosensors is that the intramolecular nature of the probe makes it more neutral by reducing its interference with the measured signaling pathways. In addition, the use of such probes resolves possible stoichiometry issues between the acceptor and donor molecules, which can be encountered when using intermolecular probes[11].

Indeed, a large number of single-chain FRET biosensors have been developed, reporting on a range of conditions within the cell (e.g., pH and calcium levels[12–14]) and on the activation level of specific signaling molecules (e.g., Rho GTPases and kinases[9,15–17]; for an updated list of available biosensors see http://www.cellmigration.org/resource/biosensors/biosen_probes.shtml).

Using FRET-based biosensors in live embryos

Although FRET-based biosensors are commonly used in experiments conducted in cell culture[9,17–19]; they have thus far been rarely used in the context of the intact organism or embryo. There are several technical obstacles to performing FRET imaging in the live animal. First, although the FRET biosensor can be overexpressed in cultured cells, in the developing embryo, high protein levels often result in abnormal development, dictating the use of low expression levels of the probe. Furthermore, the position of the cells deep within the embryonic tissue contributes to increased background fluorescence, and coupled with the low biosensor expression, makes the detection of relevant signals more challenging. Finally, the

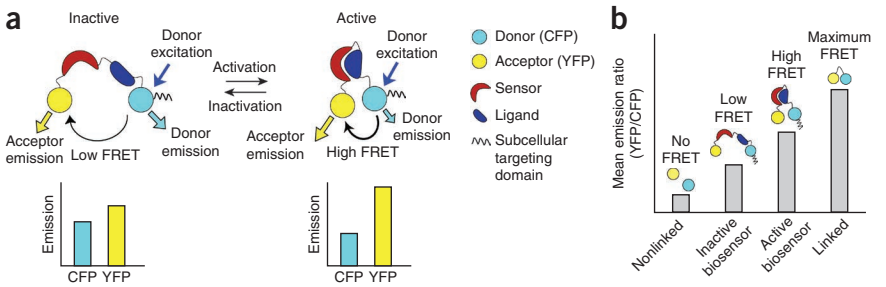

Figure 1 | The basic structure of a single-chain FRET-based biosensor. (**a**) A scheme showing the YFP and the CFP fluorophores flanking the sensor and the ligand that are connected by linkers in a chimeric molecule. Activation of the ligand module (e.g., by phosphorylation, calcium binding, GDP to GTP exchange) results in an interaction between the sensor and ligand that in turn influences the FRET efficiency. The graphs illustrate the expected relative emissions of CFP and YFP upon CFP excitation for the inactive and active states of the biosensor. (**b**) A conceptual representation of the expected differences in YFP/CFP emission ratio for different conditions: no FRET (nonlinked), low FRET level in the inactive biosensor, high FRET level in the active biosensor and maximum FRET level in the YFP-CFP tandem (linked).

variability among cells in the developing organism, as well as within a specific cell population at different time points, is higher relative to that of the more homogenous cultured cell population (see ref. 20). Performing FRET-based experiments in embryos thus requires exceedingly careful experimental setup and interpretation of the results. Indeed, given the complexities associated with FRET measurements in the live animal, the use of this technique has been limited to just a few studies in mice, *Drosophila* and zebrafish (e.g., refs. 20–26), with an evident lack of detailed protocols directing researchers how to perform FRET-based experiments in this context. The optical clarity of the zebrafish embryo allows the use of simple fluorescence microscopy for FRET measurements, whereas in other organisms two-photon microscopy is often used.

Overview of the procedure

The basic concepts underlying the application of the FRET phenomenon for measuring protein activity are presented in **Figure 1**. Specifically, activation of the biosensor results in a conformational change that alters the distance between the donor and the acceptor fluorophores (cyan and yellow fluorescent protein (CFP) and (YFP), respectively, in our case). This change in distance in turn alters the degree of energy transfer between the two molecules. This results in a change in the measured emission from donor and acceptor molecules upon donor excitation. As shown in **Figure 2**, FRET biosensors are expressed in the model system of choice (exemplified here by zebrafish embryos) and images containing the information relevant for FRET efficiency are acquired. The most commonly used method to measure the differences in FRET efficiency, and thus obtain information concerning the activation state of the biosensor, involves calculating the ratio between the YFP (acceptor) and CFP (donor) emissions upon excitation of CFP[27,28].

The aim of the protocol provided here is to assist researchers with no prior experience in FRET imaging in performing such measurements in the model system of their choice, particularly in embryos at early developmental stages. The protocol is based on previously published manuscripts in which the method was used[20,23]. We first provide instructions for introducing the probe into the embryo (using zebrafish embryos as an example); this is followed by image acquisition and the algorithm for generating ratio images. We highlight possible problems that can arise during the procedure and describe strategies to tackle them. We also provide a strategy for optimizing a particular biosensor for use in the model of choice, using the adaptation of the RacFRET biosensor to zebrafish embryos as an example. Although the protocol is focused on the use of single-chain FRET biosensors in the zebrafish model, the procedure can serve as a basis for setting up measurements with other types of FRET biosensors and other ratio imaging–based measurements in different animal and cell culture models.

Advantages and limitations

FRET measurements allow the determination of the activation state of key biochemical pathways, with the important feature of allowing such experiments in the context of the live organism under physiological conditions. The procedure is relatively fast and can be performed using comparatively simple microscopy (conventional fluorescence microscopy) and free public-domain image analysis software (ImageJ). Similarly to other methods involving fluorescence microscopy, the use of FRET-based biosensors requires that the analyzed tissue is translucent, thus limiting its application to certain developmental stages and to certain organisms;

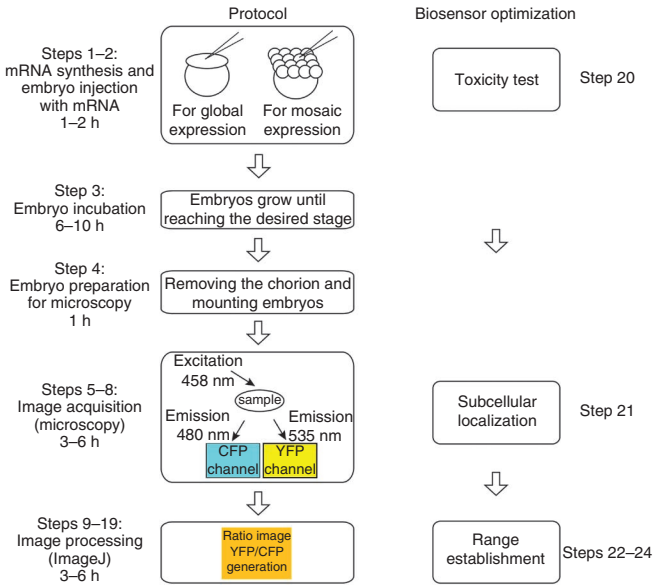

Figure 2 | Experimental flow. Key stages of the protocol (Steps 1–19) and the biosensor optimization (Steps 20–24) are outlined. mRNA is injected into a single cell at the one-cell stage for global expression or at the 16-cell stage for mosaic expression. The injected embryos are then incubated until they reach the developmental stage of interest. In the next step, the embryos are prepared for imaging procedure. During image acquisition, data sets of images of living embryos are collected. After this stage, the data can be stored until the next step. During image processing, the YFP image is divided by the CFP image to generate the YFP/CFP ratio image. To optimize the biosensor, Steps 20–24 are performed.

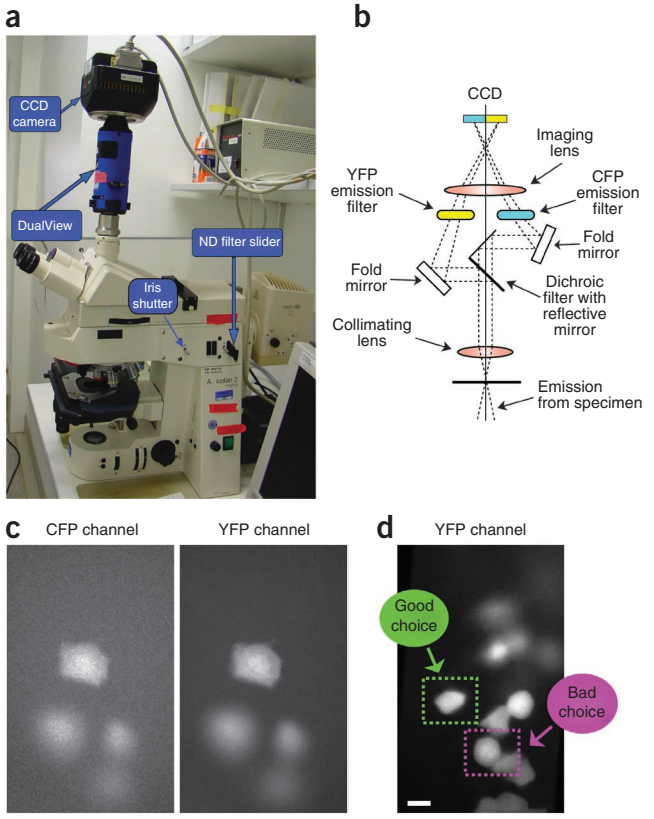

Figure 3 | Image acquisition. (**a**) Zeiss Axioplan 2 microscope is shown, with the neutral density (ND) filter slider, the iris shutter, the DualView and the charge-coupled device (CCD) camera as indicated. (**b**) A scheme showing the principle of the emission light separation in the DualView. (**c**) An example of raw images captured using DualView upon CFP excitation. CFP and YFP channels of a cell expressing YPet-SECFP tandem (encoded by mRNA derived from *YPet-SECFP-3′globin*) are shown. (**d**) The field shows labeled cells within an embryo. Good and bad choices for selection of an object are shown. In the 'bad choice' area, the presence of out-of-focus labeled cells might interfere with proper registration. Scale bar, 10 µm.

however, zebrafish embryos constitute an ideal experimental model. The expression of the probe is easily achieved in zebrafish embryos at early developmental stages (e.g., by RNA injection), but can be more complicated at later stages or when expression specific to certain tissues is required. In such cases, expression of the biosensor from a transgene should be considered.

Experimental design

Directed expression of FRET biosensors within the embryo. To achieve uniform expression of the biosensor in zebrafish embryos, we inject the mRNA containing the specific open reading frame followed by the 3′ untranslated region (3′UTR) of the *Xenopus globin* gene (*Xenopus laevis* hemoglobin, gamma A (hbg1), NM_001096347) into the yolk of one-cell stage embryos (**Fig. 2**). To label individual cells within the embryo in a mosaic pattern (thereby avoiding overlapping signal that could interfere with the measurements), we inject the mRNA into a single blastomere at the 16-cell stage (**Fig. 2**). To label zebrafish primordial germ cells (PGCs), we replace the *globin* 3′UTR with that of the *nanos* gene (*Danio rerio*, *nanos3*, NM_131878.1)[29]. Uniform expression of the biosensor, or its expression in a particular tissue or cell type in other model organisms can be achieved by using the appropriate control DNA elements in transgenic animals. Tissue-specific, promoter-driven expression can allow one to focus on a particular cell population of interest (e.g., the border cells in the *Drosophila* embryo[25]), whereas uniform expression is beneficial when the activation state of the pathway should be monitored in a wide range of cell types (e.g., determining the activation pattern of Cdc42 in whole embryos[24]). The generation of transgenic animals involves procedures that are organism specific, and these are beyond the scope of this protocol.

Image acquisition options. During FRET ratiometry measurements, the raw images are captured and then processed to obtain a ratio image that contains the information concerning protein activity (**Fig. 2**). When CFP and YFP are used as a donor and acceptor pair, the specimen is illuminated with the CFP excitation wavelength and two emission channels are recorded: CFP and YFP. In an epifluorescence microscope setup, image acquisition can be performed sequentially using a filter switching wheel[15], or simultaneously using the DualView device (**Fig. 3a**,**b**).

FRET probes are sensitive to intense illumination that can result in irreversible acceptor photo-destruction and loss of FRET[11]. Thus, the illumination must be reduced and the sample exposure to the light source minimized. To reduce illumination, neutral density (ND) filters (6–12%) are placed in front of the light source (**Fig. 3a**) and exposure time between 100 and 1,000 ms is used, depending on the signal intensity. We also recommend using the DualView device, which minimizes the time needed for data acquisition compared with using a switching wheel and thus reduces bleaching during acquisition. Accordingly, in this protocol we present the procedure using the DualView, with typical raw data images obtained using this device (**Fig. 3c**).

In the course of ratio image generation, the YFP image is divided by the CFP image, thus requiring perfect alignment of the acquired objects. DualView reduces artifacts resulting from cell shape or cell position changes when switching between the CFP and YFP channels, which is a crucial issue in cases in which these parameters change rapidly (e.g., in fast-migrating cells). However, it is important to align the DualView before the experiment and to later correct shifts that developed during the experiment (the issue of shift correction is discussed below). An important point to consider is that the acquired images should not be saturated, i.e., the image intensity level should not reach the maximum level detectable by the imaging setup. An example of how to control for this issue is shown in **Supplementary Figure 1**.

Data processing. To measure the activation state of the FRET biosensor, the YFP/CFP ratio image is generated using the raw data. The generation of the YFP/CFP ratio image requires selection of a cell to be analyzed, followed by a series of steps leading to the production of the ratio image. The selection of an area containing the cell to be analyzed is done by defining the region of interest (ROI, **Fig. 4**). Note that the ROI should contain an additional area that is to be used for the background correction, but preferably should not include additional objects, such as neighboring cells (**Fig. 4a**). In experiments done on cells in culture, practically uniform illumination can be achieved, thus allowing the definition of a specific value to be subtracted from the raw image, as this value (measured outside the object to be analyzed) is usually uniform

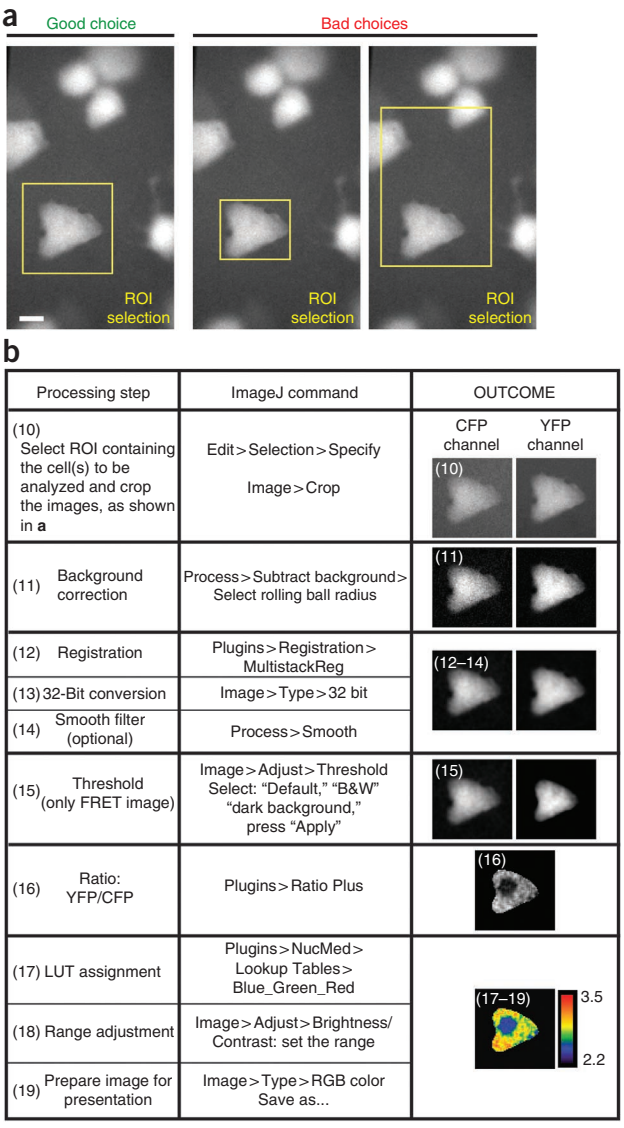

Figure 4 | Ratio image generation procedure. (**a**) Examples for ROI selection: 'good choice' refers to a selected region that includes sufficient area for background subtraction, while it does not include additional objects that might affect proper registration. These considerations, when ignored, are demonstrated under 'bad choices'. (**b**) The procedure for ratio image generation using the ImageJ software. The individual processing steps and respective ImageJ commands are listed, and the images corresponding to the processing steps are shown at right. The numbers listed in parentheses correspond to the step numbers in the PROCEDURE.

throughout the field. In the case of measurements within embryos, light scattering and nonuniform emission from the embryonic tissue (due to differences in tissue thickness, variability in the number of labeled cells in specific regions and so on) result in substantial differences in background values within the field, thereby making it difficult to define the value to be subtracted. These complications should thus be addressed using specific algorithms for background subtraction (e.g., the rolling ball algorithm, http://rsbweb.nih.gov/ij/docs/guide/userguide-26.html#toc-Subsection-26.14).

It is often the case that two images obtained in YFP and CFP emission channels are not properly aligned because of a few pixels shifts. These shifts can be corrected during image processing by image registration, a step that requires the analyzed cells to be positioned in the middle of the field of view and preferably isolated from other cells. The presence of objects in the vicinity of the cell to be analyzed, especially if these are out of focus, could interfere with proper image registration during processing, thereby resulting in artifacts in the processed image (**Fig. 5**). A representative example for good and bad choices of cells to be analyzed is shown in **Figure 3d**. The green arrow points at an isolated cell, which is a good choice, whereas the magenta arrow points at a group of cells, which would not be an ideal selection because of out-of-focus cells in close proximity to the measured object. The single steps for data processing are outlined in the PROCEDURE and in **Figure 4b**. Sample raw data images of the CFP and YFP emission channels for practicing the procedure using ImageJ are provided in **Supplementary Data 1** (RawCFP) and **Supplementary Data 2** (RawYFP).

Basic controls for FRET ratiometric imaging. Proper controls are important for the initial setup and optimization of FRET measurements and are essential for establishing the appropriate imaging conditions in a given experimental setup. In this step, the YFP/CFP emission ratio is determined and compared between two conditions: the absence of FRET ('nonlinked' in **Figs. 1b** and **6a**,**b**) and the maximum FRET ('linked' in **Figs. 1b** and **6a**,**b**), thus providing the minimum and maximum value range in the experiment. In the nonlinked control, equal CFP and YFP fluorophores are expressed (performed by injection of equal molar amounts of mRNAs containing the same 3′ and 5′ UTR elements) and serve to determine the YFP/CFP ratio in the absence of FRET. In the linked control, the YFP-CFP tandem is expressed and serves to define the highestYFP/CFP ratio. Determining the difference between the values measured for these two controls will also allow possible artifacts associated with FRET ratiometry to be detected, such as incorrect image registration or loss of FRET as a result of bleaching (see TROUBLESHOOTING). The lack of such artifacts is manifested in a uniform pattern of low or high FRET ratios within the cells of the nonlinked and linked probes, respectively.

Choice of fluorophores. Most FRET-based experiments use CFP and YFP as donor and acceptor flurophores, respectively, for the energy transfer, as this combination offers high quantum yield of the acceptor protein[30], thus increasing sensitivity. Different variants of these proteins showing improved energy transfer have been

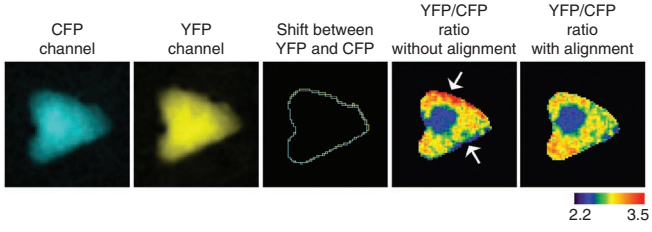

Figure 5 | Ratio imaging artifacts. Shown is an artifact resulting from the ratio calculation of misaligned CFP and YFP images. The CFP and YFP images of a somatic cell expressing the RacFRET biosensor are shown (the images are those shown in **Fig. 4**). The contours of the CFP and YFP images demonstrate the shift between the two channels. YFP/CFP ratio images derived from misaligned and from properly aligned YFP and CFP images are shown. Arrows indicate the areas at the edges where the artificial YFP/CFP ratio signal that resulted from the shift between the YFP and CFP images is more pronounced.

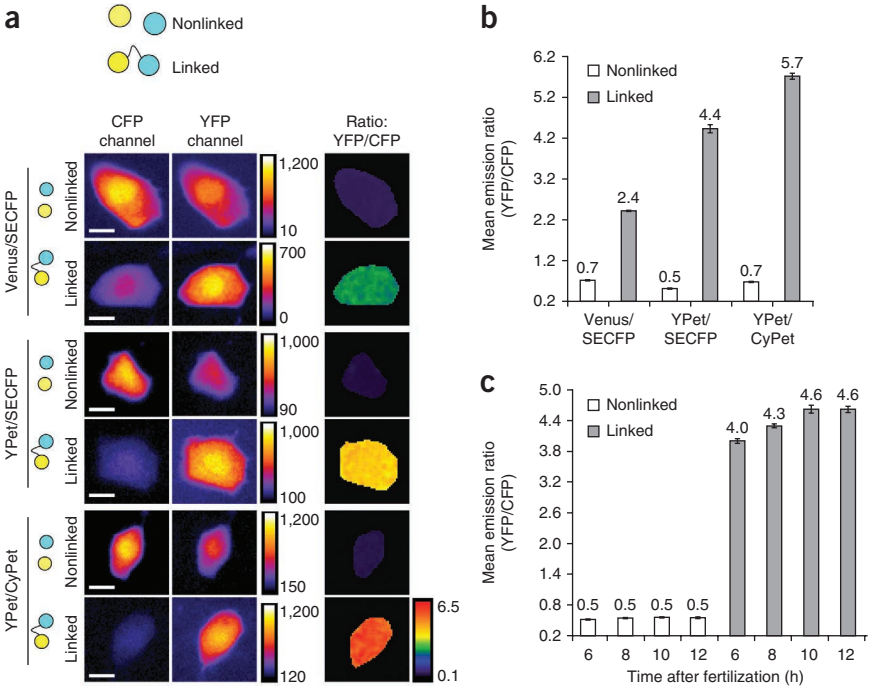

Figure 6 | Basic controls used during FRET imaging setup. (**a**) Representative somatic cells expressing linked or nonlinked YFP/CFP combinations are shown. Three combinations of CFP and YFP molecule variants are used: Venus/SECFP, YPet/SECFP and YPet/CyPet. For each combination, the raw images of the CFP and the YFP channels, as well as the corresponding YFP/CFP ratio, are shown. The CFP and the YFP emission intensities are presented in the 'fire' pseudocolor mode of ImageJ and are set to the same range for each construct to show the typical differences between the intensities observed in the YFP and CFP channels in the absence and in the presence of FRET. The YFP/CFP ratio is presented using the 'Blue_Green_Red' pseudocolor mode. (**b**) A graphical representation of the results is shown in **a** as measured for the entire cell. (**c**) A graph showing the time-dependent increase in YFP/CFP ratio in somatic cells of the developing embryos observed for the YPet-SECFP tandem. To label individual somatic cells, single blastomeres were injected at 16-cell stage zebrafish embryos with mRNA for the following: equal amounts of *Venus-3'globin* and *SECFP-3'globin* (B441 and B758; nonlinked) or *Venus-SECFP-3'globin* (B760; linked) for the Venus/SECFP combination; equal amounts of *YPet-3'globin* and *SECFP-3'globin* (B757 and B758; nonlinked) or *YPet-SECFP-3'globin* (B761; linked) for the YPet/SECFP combination; or equal amounts of *YPet-3'globin* and *CyPet-3'globin* (B757 and B759; nonlinked) or *YPet-CyPet-3'globin* (B762; nonlinked) for the YPet/CyPet combination. For all RNAs, the same RNA regulatory sequences (3' and 5' UTRs) were used. Scale bar, 10 µm. Error bars show s.e.m.

developed[31]. Here we show the use of three combinations of CFP and YFP variants, connecting the fluorophores with a specific linker (13 aa) in the zebrafish system (**Fig. 6a**,**b**). YPet has improved brightness and photostability[32,33], and as previously shown *in vitro*[31], it yielded the best FRET signal when used in combination with CyPet. The high FRET values observed for this combination, however, are associated with a very strong reduction in CFP emission (**Fig. 6a**), thereby potentially increasing measurement errors. As a rule, we try to obtain a signal level within the cell that is at least double that of the background, a point that is more difficult to achieve using the YPet-CyPet combination. Comparing the three combinations tested, we would thus recommend using the YPet-SECFP pair, but would encourage retesting this point in the specific experimental setup.

We observe an increase in FRET in the linked control YFP-CFP tandem molecules during the first day of development (**Fig. 6c**), in particular between 6 and 10 h after injection. This general increase in FRET signal should be considered when comparing FRET values between different time points.

Controlling for biosensor-induced artifacts. The expression of the FRET biosensor should have no effect on cellular processes, as judged by proper embryonic development and normal cell behavior. Thus, when expressing biosensors in a particular tissue or a group of cells, the behavior of the tissue and the cells should be compared with that observed in embryos injected with RNA, which does not encode protein domains that could affect proper development (e.g., GFP alone). For example, in the case of migrating cells, the proper behavior of the cells during migration, as well as their arrival at the correct location within the embryo should be examined[20]. **Figure 7a** shows the scheme for the RacFRET biosensor used here as an example.

To test the possible toxicity of the RacFRET biosensor, we followed the development of the zebrafish embryo, expressing the protein during the first 24 h after fertilization. As shown in **Figure 7b**, the development of embryos expressing the biosensor appeared normal as compared with nontreated embryos.

Subcellular localization of the RacFRET biosensor. The subcellular localization of the FRET biosensor for a specific protein should be similar to that of the endogenous protein. To examine this point, we compare the subcellular distribution of the mCherry fusion protein (e.g., Rac, in this case) and the corresponding FRET biosensor. We have previously described the principle for the subcellular targeting of RacFRET biosensor in PGCs (see ref. 20) and we show here a similar procedure for somatic cells. **Figure 7c** shows the scheme of the C-terminal (CT) targeting domain from the original biosensor (Rac1-CT) and the two modifications we introduced to this domain (NoNLS and NoCT). In contrast with the subcellular localization of the mCherry-Rac1 fusion protein (**Fig. 7d**), the unmodified RacFRET biosensor was found to be localized primarily to the nucleus with weak localization to the cell membrane (**Fig. 7d**). Mutating or deleting the nuclear localization signal at the C terminus of the protein (**Fig. 7c**) resulted in localization of the biosensor that appeared more similar to that of the mCherry-Rac1 fusion protein. The RacFRET construct lacking the C terminus of the protein (RacFRET-NoCT) showed subcellular localization most similar to that of the mCherry-Rac1 protein (**Fig. 7d**) and was thus used for the subsequent studies. The description above relates to specific subcellular targeting sequences (prenylation and nuclear localization); when using other FRET constructs, one might have to consider other types of localization motifs.

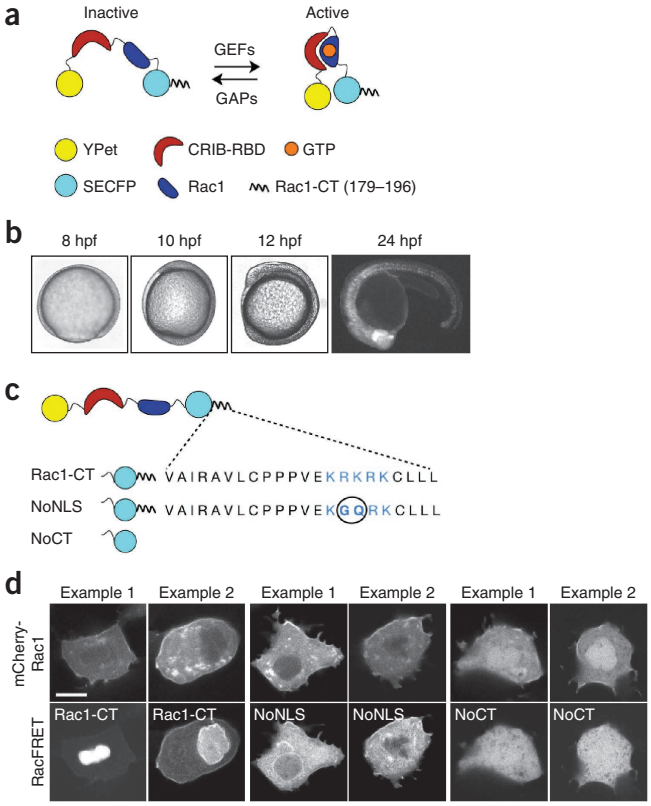

Figure 7 | Adaptation of the RacFRET biosensor for measurements in zebrafish embryos. (**a**) Domain structure of the RacFRET biosensor. (**b**) Zebrafish embryos expressing the RacFRET-noCT biosensor. Bright-field images of early developmental stages and a fluorescent image of a 1-d-old embryo are shown. (**c**) Schematic representation of the C-terminal (CT) targeting sequence in the original RacFRET biosensor and the two C-terminal modifications used in this study. The nuclear localization signal (NLS) in the Rac1-CT is highlighted in blue. The mutations eliminating the NLS are circled. (**d**) Subcellular localization of the mCherry-Rac1 (upper panels), and three C-terminal variants for RacFRET biosensors expressed in the somatic cells (lower panels). Two representative cells for each construct are shown. To achieve uniform expression of the biosensor, mRNA for *RacFRET-NoCT-3′globin* (B763) was injected into the yolk at the one-cell stage (in **b**). To monitor Rac1 subcellular localization in individual somatic cells in the embryo, mRNA for *mCherry-Rac1-3′globin* (B800) was injected into a single blastomere at the 16-cell stage (in **d**, top). To monitor the effect of C-terminal modifications on RacFRET subcellular localization in somatic cells, the following mRNAs were injected into a single blastomere at the 16-cell stage: for *RacFRET-RacCT-3′globin* (B782, bottom, two left images), *RacFRET-noNLS-3′globin* (B783, bottom, two middle images) and for *RacFRET-noCT-3′globin* (B763, bottom, two right images). The images were acquired between 8 and 10 h after fertilization. Scale bar, 10 μm.

Establishing the activity range of the biosensor. To correctly interpret the results, it is important to determine the differences in YFP/CFP emission ratios between the biologically active and inactive states of the biosensor, thus establishing the relevant range of activation. Using the YFP/CFP ratio in the absence of FRET in the nonlinked control cannot serve as the proper low value, as a certain level of FRET occurs in the biosensor in even its biologically inactive state (**Fig. 1b**). In general, the FRET construct should be mutated such that it reports on the maximum or minimum possible activation states. Alternatively, the determination of these values can be achieved through coexpression of other molecules that activate or inactivate the protein. To exemplify such a procedure, we establish the range between the inactive and active states for the RacFRET biosensor using the following strategy: to measure the YFP/CFP ratio corresponding to the inactive state of the RacFRET biosensor, we coexpress the RacFRET biosensor with a guanine nucleotide exchange factor (GEF) inhibitor, the dominant-negative Rac1N17 mutant (**Fig. 8a**,**b**). We have previously shown that using different concentrations of Rac1N17 results in a corresponding change in the observed activation level[20]. To measure the ratio corresponding to the most active state of the RacFRET biosensor, we introduce the G12V substitution in the coding region of Rac within the FRET biosensor (**Fig. 8a**,**b**). This mutation eliminates the GTPase activity of Rac within the biosensor, rendering it 'locked' in the active conformation[15,34]. The functionality of a biosensor can be further validated by expressing a known activator of the protein. For example, in the case of the RacFRET construct coexpressing the RacFRET biosensor and the DH-PH domain of Tiam1—a functional unit of the specific GEF for Rac—elevates the detected activation state of the biosensor (**Fig. 8c**,**d**).

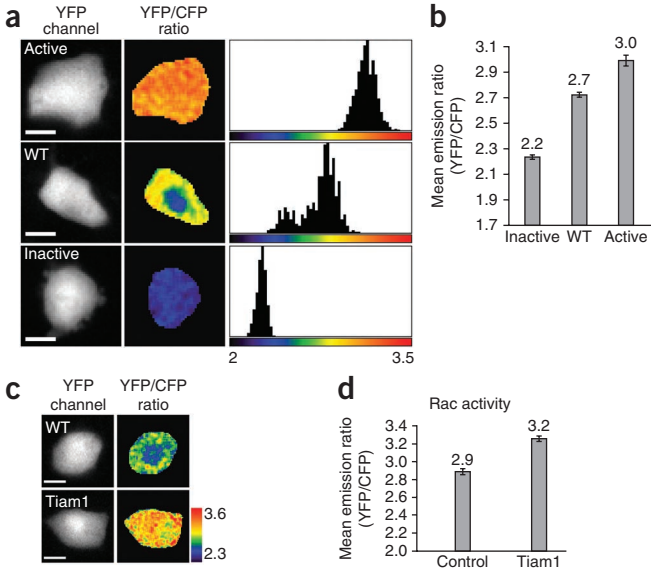

Figure 8 | Controls used for measuring Rac activity. (**a**) The span of RacFRET biosensor activity ranging from the active to the inactive state is established. Representative somatic cells expressing RacV12-FRET used to measure the constitutively active state of the biosensor (upper panels), RacFRET to measure wild-type (WT) situation (middle panels) and RacFRET together with Rac1N17 to measure the inactive state of the biosensor (lower panels) are shown. To label individual somatic cells, single blastomeres of zebrafish embryos at the 16-cell stage were injected with the *RacV12FRET-noCT-3′globin* mRNA (B787, active), *RacFRET-noCT-3′globin* (B763, WT) and a mixture of *RacFRET-noCT-3′globin* together with *Rac1N17-3′globin* mRNAs (B763 and B784, Inactive). The imaging was performed 8 h after fertilization. The histograms show the pixel distribution within the ratio image. (**b**) The graph shows the mean YFP/CFP emission ratio for the entire cells. At least 20 cells were analyzed for each sample. (**c**) The effect of DH-PH domain of Tiam1 on Rac activity. To measure the effect of DH-PH domain of Tiam1 on RacFRET activation state, single blastomeres at 16-cell stage embryos were injected with the *RacFRET-noCT-3′globin* mRNA (B763, WT) or a mixture of *RacFRET-noCT-3′globin* and *zTiam1-DH-PH-3′globin* mRNAs (B763 and B784, Tiam1). (**d**) The graph shows the mean emission ratio YFP/CFP for the entire cell. Scale bar, 10 μm. Error bars show s.e.m.

MATERIALS

REAGENTS

DNA templates for mRNA synthesis (general requirements)

- Biosensors
- Donor control construct
- Acceptor control construct
- 'Linked' control construct
- Constructs for determining activity range of biosensor
- Constructs for checking biosensor localization (see **Figs. 1a** and **7a** for a schematic figure of the general structure of these constructs and **Supplementary Table 1** for details of specific constructs used as examples in this protocol.)
- mMessage mMachine SP6 or T3 kits, depending on the promoter used for *in vitro* transcription (Ambion, cat. nos. AM1340 and AM1348)
- Zebrafish (adult zebrafish lines of AB and TL phenotypes were obtained from the fish facility at the Max Planck Institute for Molecular Cell Biology and Genetics in Dresden, Germany. Media and general handling procedures can be found at http://zfin.org/zf_info/zfbook/cont.html#cont2 (refs. 35,36).)

EQUIPMENT

Fish handling

- Agarose molds with slots to accommodate the embryos, glass slide, plastic rings, low-melting agarose or any other mounting system routinely used for imaging (http://zfin.org/zf_info/zfbook/cont.html#cont2)
- Dumont 5 forceps (Fine Science Tools, cat. no. 11252-20)

Imaging equipment

- Confocal microscope (we use the Zeiss LSM 710 upright confocal microscope for determining the precise localization of protein fusions in the context of the live organism; see EQUIPMENT SETUP)

FRET imaging equipment

- Fluorescence microscope for FRET data acquisition (we use Zeiss Axioplan 2 equipped with the DualView Imager (Visitron Systems, http://www.visitron.de/Products/Microscope_Peripherals/Image_Splitter/image_splitter.html) and cooled CCD camera (RD sliding spot from Diagnostic Instruments) controlled by the Metamorph software)
- Metamorph software (Molecular Devices)
- Objective for FRET measurements (Plan-Apochromat ×40/1.0 DIC water-dipping lens; we have examined the Zeiss water-dipping lens ×40/0.8 W, Achroplan, which is a cheaper option and could not detect significant differences when compared with the Apochromat lens.)
- Ultraviolet (UV) illumination system (we use mercury short arc 100 W)
- Neutral density (ND) 6% transmission filter fitted before the UV illumination source (**Fig. 3a**)
- YFP filter cube (used to find the labeled cells) with Exciter 500AF25 (Omega Optical, XF1068), Dichroic 525DRLP (Omega Optical, XF2030), Emitter 545AF35 (Omega Optical, XF3074)
- FRET filter cube for use with DualView (Exciter 440AF21 (Omega Optical, XF1071); and Dichroic 455DRLP (Omega Optical, XF2034). The emission filter is removed.)
- DualView (equipped with 505dcxr beam splitter, ET 480/40m CFP emission filter and ET 535/40 YFP emission filter)
- ImageJ software (http://rsbweb.nih.gov/ij/)

EQUIPMENT SETUP

Confocal setup We use Zeiss LSM 710 upright confocal microscope to determine the precise localization of protein fusions. The use of a confocal microscope for this purpose is especially important in the context of the live organism, where signal from other cell layers can interfere with precise determination of the subcellular localization. The microscope settings depend on the specific sample, the intensity of the signal and the microscope used. We used the following settings for the Zeiss upright LSM 710 system.

- Lasers used for excitation: 488 nm 6%, 561 nm 8%
- Objective: water-dipping lens ×63/1.0 W plan-Apochromat M27
- Filter settings for emission detection, Channel 1 (FRET biosensor localization detection): 500–550 nm
- Filter settings for emission detection, Channel 2 (mCherry-Rac localization detection): 580–700 nm
- Channel 2 Image properties: 512 × 512 pixels, 8 bit
- Scan mode: plane
- Averaging: Line 2
- Master gain for Channel 1: 800
- Master gain for Channel 2: 800
- Digital gain, Channel 1: 1
- Digital gain, Channel 2: 1
- Digital offset, Channel 1: 0
- Digital offset, Channel 2: 0
- Pinhole, Channel 1: 70 µm
- Pinhole, Channel 2: 70 µm (1 Airy unit)
- Beam splitters: MBS: MBS 488/561

FRET ratiometric imaging setup Before imaging, ensure that the ND filter is positioned in the illumination path (**Fig. 3a**). Use an ×40 magnification objective. If the signal is weak, increase the binning. Align the DualView splitter according to the instructions provided by manufacturer. The DualView is used in combination with the FRET filter cube without the emission filter. If a DualView is not available, use CFP and FRET filter cubes to acquire the CFP and YFP emission channels sequentially.

Image processing software To download and install ImageJ software, use the link http://rsbweb.nih.gov/ij/download.html and follow the instructions. The current ImageJ version used here is 1.43 for MacOS and the instructions below relate to this version. Note that some of the plug-ins, namely TurboReg, MultiStackReg v1.45, Calculate Fura-2 (calcium) Ratios ('Ratio Plus'), and Lookup Tables (Download the 'NucMed') are not included in the basic ImageJ package and should be downloaded from the plug-ins page in the ImageJ website (http://rsbweb.nih.gov/ij/plugins/). While processing the data, it is useful to save intermediate steps, as the software does not perform this step automatically. The processing sequence for generating YFP/CFP ratio image is outlined in **Figure 4b**.

PROCEDURE

Introduce controls into embryos for setting up imaging conditions ● TIMING 12–17 h

1| Use the appropriate DNA constructs as templates to synthesize capped mRNA; we use the mMessage mMachine kit according to the manufacturer's instructions. To set up initial imaging conditions, the following constructs are needed: the donor control construct, the acceptor control construct and the linked control construct. The acceptor and donor molecules in the control constructs should be identical to those used in the biosensor construct. For example, for setting up the conditions for the biosensor A422.*RacFRET-3'nos*, use B757.*YPet-3'globin* and B758.*SECFP-3'globin* for the nonlinked control and B761.*YPet-SECFP-3'globin* for the linked control (**Supplementary Table 1**), where SECFP and YPet are the donor and acceptor fluorophores, respectively.

■ **PAUSE POINT** Capped mRNA can be stored at −80 °C. In our hands, aliquots of capped mRNA stored at −80 °C could be used more than 5 years after synthesis.

2| Inject equimolar amounts of the acceptor and donor mRNAs together (nonlinked negative control) into about 30 embryos, and inject an equivalent total amount of the linked mRNA (positive control) into another 30 embryos. The concentrations for the mRNAs described here are provided in **Supplementary Table 1**. For other FRET sensors, one has to determine the mRNA amount to be injected on the basis of the signal level and possible deleterious effects on embryonic development. Inject zebrafish embryos using standard methods, as previously described[36].

▲ CRITICAL STEP These controls allow imaging conditions to be established in a given experimental system. The difference between the acceptor/donor emission ratio values for the negative (nonlinked, absence of FRET) and positive (linked, presence of FRET) controls provides the range within which the ratio values for different activation states of the biosensors should reside.

3| Incubate embryos at 25–30 °C until they reach the desired developmental stage. We were able to measure FRET about 6 h after mRNA injection.

4| Dechorionate 10–15 embryos from each batch of injections with forceps using standard methods, e.g., http://wiki.zfin.org/display/prot/Removing+Embryos+from+Their+Chorions, and mount the embryos as described in http://wiki.zfin.org/display/prot/ZFIN+Protocol+Wiki and ref. 35.

Acquire images ● TIMING 3–6 h

5| Use the appropriate filter cube to search for cells to image, e.g., YFP filter cube for a YFP/CFP acceptor/donor pair, as is described here. The image-acquisition setup is presented in **Figure 3a**,**b**.

▲ CRITICAL STEP To avoid bleaching and loss of FRET[11] during acquisition, make sure that the light intensity is reduced before starting the experiment. This can be done by introducing the ND filter (**Fig. 3a**) and/or by reducing the power to the light source.

6| Find isolated cells expressing the fluorescent protein; position them to the middle of the field of view and focus. Optional: if possible in the specific microscope setup, use the iris to reduce the stray light, thereby improving image quality (**Fig. 3a**).

7| To acquire FRET data using the DualView, switch to the FRET filter cube.

! CAUTION Do not look into the ocular when the FRET filter cube is active, as an emission filter is not present in this cube; the light intensity is extremely strong and potentially harmful to eyes.

8| Acquire CFP and YFP emission images upon CFP excitation. In this way, image 20–30 cells for each sample (this is a good number to get an estimate for noise and fluctuations).

▲ CRITICAL STEP When acquiring images from zebrafish embryos at early stages of development (6–12 h after fertilization), make sure that the incubation time is similar for the different experimental samples to avoid artifacts stemming from a general increase in the YFP/CFP emission ratio during development (**Fig. 6c**).

■ PAUSE POINT The raw images can be stored in the original file format generated by the microscope software and analyzed at a later time point.

? TROUBLESHOOTING

Image processing: YFP/CFP ratio image generation algorithm ● TIMING 3–6 h

9| Open the raw CFP and YFP images in the ImageJ software. Steps 10–14 should be performed both for YFP and CFP images.

▲ CRITICAL STEP We describe the use of the open source software, ImageJ. However, processing (**Fig. 4**) can alternatively be performed using commercial software (e.g., Metamorph). Please note that while processing the data, it is important to save intermediate steps, as the software does not do it automatically.

10| *ROI selection*: use the YFP image to select the ROI containing the object to be processed. This is done by drawing a rectangle using the 'rectangular selection' ImageJ icon, or by specifying a region using the 'Edit→Selection→Specify' command from the ImageJ menu. To store the ROI, select 'Analyze→Tools→ROI manager', press 'Add', and then a number will appear in the ROI manager box. Switch to the CFP image and double-click the number in the ROI manager box to get the same ROI positioned on the CFP image. Crop both images (CFP and YFP) using the command 'Image→Crop' from the ImageJ menu.

▲ CRITICAL STEP When drawing an ROI, leave a background area around the cell to allow for background correction. Avoid additional objects within the ROI. **Figure 4a** shows good and bad examples of ROI selection.

11| *Background correction*: select 'Process→Subtract background' from the ImageJ menu and proceed with all boxes unchecked in the dialog box. Here we use the rolling ball algorithm with a rolling ball radius range of 50–200 (the radius of the rolling ball should not be smaller than that of the largest object in the image). For the sample images provided (**Supplementary Data 1** (RawCFP) and **Supplementary Data 2** (RawYFP)), use a rolling ball radius of 50. Apply this to both images.

12| *Registration*: the raw CFP and YFP images are often misaligned with a shift of a few pixels between the two images, resulting in severe artifacts. Select 'Plugins→Registration→MultiStackReg' (or 'Plugins→MultiStackReg') from the ImageJ menu to align two images or two stacks of a time-lapse movie. In the 'MultiStackReg' dialog box, select the CFP image (stack 1)

as a reference stack ('use as reference' in action 1) and align the YFP image to it ('Align to First Stack' in action 2). Select 'Rigid Body' as a transformation method.

13| *32-bit conversion*: This is necessary for the subsequent thresholding in Step 15. Select the command 'ImageType→32 bit' from the ImageJ menu. Apply this to both images.

14| *Smooth filter*: This step is recommended to improve image quality by reducing the noise. Select 'Process→Smooth' from the ImageJ menu. Apply this to both images.

15| *Threshold*: This step should be applied exclusively to the YFP image, converting the background pixels to 'not a number' (NaN). It allows elimination of artifacts in ratio image stemming from the background noise. Select 'Image→ Adjust→ Threshold' from the ImageJ menu. Select the following parameters: 'Default', 'B&W' and 'Dark Background'. Press 'Apply'. An icon will appear with the sign 'Set Background Pixels to NaN'. Press 'OK'.

16| *Ratio YFP/CFP*: Select 'Plugins→ Ratio Plus' from the ImageJ menu to generate a YFP/CFP ratio image. Choose the YFP image as 'Image1' and the CFP image as 'Image2' and press 'OK'.

17| *Lookup table (LUT) assignment*: To generate a color-coded image we use the Blue_Green_Red lookup table. Select 'Plugins→NucMed→Lookup tables' from the ImageJ menu'. Select 'Blue_Green_Red' as a lookup table name.

18| *Range adjustment*: Process all the images obtained in Step 8 as described in Steps 9–17, and calculate the mean activation level for each sample. Select 'Image→Adjust→Brightness/Contrast' from the ImageJ menu. Press 'Set' in the 'B&C' dialog box and define the range between the active and inactive states using the mean values obtained with images for positive and negative controls. When setting the range initially, use the mean values for the linked control images and the nonlinked control images. After subsequent optimization of a particular FRET biosensor (Steps 22–24), the range is refined using the mean values obtained for the active and inactive controls; this is the range that is used in subsequent experiments using that biosensor (Step 25). In the examples provided here for the RacFRET biosensor, the range is 2–3.5 (**Fig. 8a**,**b**).

19| To save an image for presentation purposes, convert it to RGB. Select 'Image→Type→RGB color' from the ImageJ menu and save the image as a TIFF file. Note that the quantitative information within the ratio image is lost when it is converted to 'RGB'; therefore, we recommend saving the original YFP/CFP ratio image before the RGB conversion.
? TROUBLESHOOTING

Determine the toxicity of the specific biosensor ● TIMING 1–2 d
20| Synthesize and inject the mRNA encoding the FRET biosensor into the yolks of one-cell-stage zebrafish embryos as described in Steps 1–3. To determine the optimal concentration necessary, inject different amounts of mRNA, ranging from 100 to 500 pg per embryo. We typically evaluate two or three different concentrations within the indicated range. Monitor the embryos and tissues expressing the biosensor during development to determine the expression level that provides sufficient signal for imaging, while not affecting cell behavior, tissue differentiation and embryonic development. **Figure 7b** shows an example of normally developed zebrafish embryos expressing the RacFRET biosensor.

Confirm proper subcellular localization of the biosensor ● TIMING 1–2 d
21| Synthesize mRNA for the localization control (e.g., a fluorescently tagged fusion protein) and co-inject with the FRET biosensor mRNA into one-cell-stage zebrafish embryos as described in Steps 1–3. For each construct, inject about 30 embryos with 100–400 pg mRNA per embryo. Inject two or three different amounts of mRNA within this range, using equimolar amounts of the RNA encoding localization control and the FRET biosensor. Compare the subcellular localization of the control protein with that of the FRET biosensor, preferentially using confocal microscopy. **Figure 7d** shows the subcellular localization of RacFRET biosensors expressed in somatic cells of zebrafish embryos.
▲ CRITICAL STEP When the subcellular localization of the FRET biosensor does not match that of the fusion protein, additional cloning steps might be required to optimize the biosensor. The time required for these steps varies, depending on the particular biosensor used, and could take several weeks.

? TROUBLESHOOTING
Establishing the range between the active and inactive states of the biosensor ● TIMING 1–2 d
22| Design controls that inactivate or hyperactivate the biosensor. For RacFRET, we have used the following controls (**Supplementary Table 1**): active = RacV12-FRET (B787); inactive = wild-type RacFRET coexpressed with Rac1N17

(B763 together with B784). As an additional control for responsiveness of RacFRET, one can coexpress the DH-PH domain of Tiam1 that should activate the biosensor.

23| Synthesize mRNAs for three different samples: the wild-type RacFRET, the active (RacV12-FRET) control and the inactive (RacFRET + Rac1N17) control. Inject mRNA into a single blastomere of 16-cell-stage zebrafish embryos as described in Step 2. In addition, synthesize and co-inject mRNAs encoding the wild-type RacFRET and the DH-PH domain of Tiam1 (B763 + B786) to measure the activation of RacFRET by Tiam1. Inject mRNA amounts for the biosensor as determined in Step 20 into at least 30 embryos for each sample. The optimal amounts for Rac1N17 mutant and DH-PH of Tiam1 are determined by trying two or three concentrations within the range of 100–400 pg per embryo. The amounts we used in our setup are indicated in **Supplementary Table 1**.

24| Measure the YFP/CFP emission ratio values from 20 to 30 cells as described in Steps 5–19. The YFP/CFP emission ratio values are highest for the active control and lowest for the inactive control, whereas the YFP/CFP emission ratios obtained with the wild-type sample should be in between those two values.

Using the optimized biosensor in experiments ● TIMING 1–2 d

25| To conduct experiments, repeat Steps 1–19 with the optimized biosensor and obtain measurements under control (wild type) or manipulated conditions (if relevant). Ensure that activation levels fall within the range measured in Step 24. Set the range in Step 18 according to the values obtained in Step 24 for the active and inactive states of the biosensor.

? TROUBLESHOOTING

Troubleshooting advice can be found in **Table 1**.

TABLE 1 | Troubleshooting table.

Step number	Problem	Possible reason	Solution
8	Insufficient signal level in the CFP image	Low expression level of the biosensor	Increase binning, use longer exposure times or express higher levels of the biosensors when possible
	Loss of FRET in the biosensor, or in the YFP-CFP tandem protein (this is identified as an exceptionally low FRET ratio relative to the value expected from the past experience. In the setup stages, CFP and YFP emission levels similar to those obtained from the nonlinked control indicate lack or loss of FRET)	Intense illumination can result in the loss of FRET[11]	Minimize the illumination using a neutral density filter or by reducing the power of the fluorescent source when possible
19	Artifact in the ratio image manifests as very high and very low values that often appear at the edges of the analyzed object (**Fig. 5**)	A shift between YFP and CFP images, which was not properly corrected during the registration step (Step 12 in this procedure). Misalignment is usually caused by registration problems as a result of the presence of additional objects in a field of view, or due to poor alignment of the DualView. Another reason for poor alignment could be strong background signal that was not properly corrected	Check that the background in both channels is properly subtracted and repeat the registration step. In case of additional out-of-focus objects, exclude these by selecting smaller ROIs. Check the alignment of the DualView
	Values in the ratio image are much lower than expected	The CFP and YFP images were swapped	Verify the identity of the images and repeat the ratio generation procedure
21	Subcellular localization of the biosensor does not match that of the mCherry fusion of the corresponding protein	The FRET biosensor size or the presence of cryptic subcellular protein sequences could affect its localization	Identify and mutate the putative localization protein sequences if possible. Otherwise, use the version that is uniformly distributed within the cell

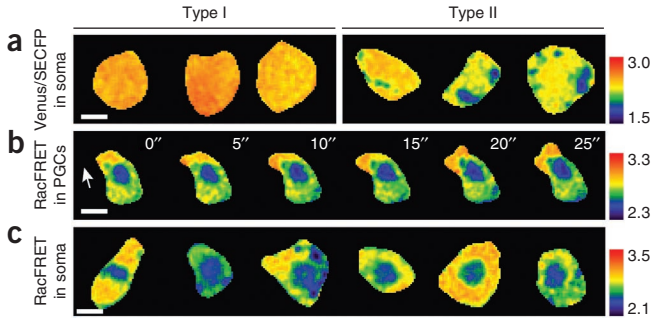

Figure 9 | Examples of FRET images in zebrafish. (**a**) Representative YFP/CFP ratio images of individual somatic cells expressing Venus-SECFP tandem are shown. Type I refers to the cells with the uniform FRET ratio pattern, whereas Type II refers to the cells with a nonuniform FRET ratio pattern. *Venus-SECFP-3′globin* mRNA (B760) was injected into a single blastomere of 16-cell-stage embryos and the imaging was performed at 8 h after fertilization. (**b**) Rac activation in migrating primordial germ cells (PGCs). To express the RacFRET biosensor in PGCs, *RacFRET-noCT-3′nos* mRNA (A422) was injected into one-cell-stage zebrafish embryos and the imaging was performed at 9 h after fertilization. The arrow indicates the direction of migration; images were captured at 5-s (″) intervals. (**c**) Variations in Rac activation patterns observed in the somatic cells in zebrafish embryos at 9 h after fertilization. To express RacFRET biosensor in somatic cells, *RacFRET-noCT-3′globin* mRNA (B763) was injected into single blastomeres of 16-cell-stage zebrafish embryos and the imaging was performed at 9 h after fertilization. Individual somatic cells are shown. Scale bars, 10 μm.

● TIMING

Step 1, mRNA synthesis and purification: 4 h
Step 2, Embryo injection: 1–2 h
Step 3, Embryo incubation: 6–10 h or longer, depending on the developmental stage of interest
Step 4, Embryo preparation for microscopy: 1 h
Steps 5–8, Imaging: 3–6 h
Steps 9–19, Data processing: 3–6 h
Step 20, Checking the toxicity of the biosensor: 1–2 d
Step 21, Confirming proper subcellular localization or the biosensor: 1–2 d
Steps 22 and 23, Setting up the range between the active and inactive states of the biosensor: 1–2 d
Step 24, Conducting the experiment: 1–2 d

ANTICIPATED RESULTS

An example of how the described procedure is used in the context of a specific scientific question is the study of the role of Rho GTPases in germ cell migration[20]. In this work, a procedure similar to the one described in this protocol was used for measuring the activation state of Rac1 and RhoA using optimized biosensors. In this case, in which the focus was on PGCs, the corresponding biosensors were expressed preferentially in those cells.

Typical results obtained with different FRET biosensors are shown in **Figure 9**. The expected pattern from the maximum FRET-control biosensor is a uniform signal (**Fig. 9a**). However, we find subpopulations of somatic cells that show areas of low YFP/CFP ratio values (**Fig. 9a**). These could represent organelles in which the conditions (e.g., pH) affect FRET efficiency[37]. It is therefore essential to compare the activation patterns detected with a particular biosensor with those obtained with control biosensors. For a FRET pattern to reflect a molecule's real activation pattern, there should be a clear difference between the pattern obtained with the experimental biosensor and that with the control biosensors (**Fig. 8a**).

An example of an activation pattern measured by FRET is shown in **Figure 9b**. Here, elevated Rac activity in a migrating PGC is detected at the cell front. **Figure 9c** shows examples of the Rac activity pattern that we observe in somatic cells of a zebrafish embryo.

Note: Supplementary information is available via the HTML version of this article.

ACKNOWLEDGMENTS This work was supported by grants from the Deutsche Forschungsgemeinschaft (DFG) and the Max Planck Society. We thank M. Reichman-Fried for critical reading of the manuscript and E.-M. Messerschmidt for technical assistance. We also thank M. Matsuda and P. Daugherty for sharing the constructs.

AUTHOR CONTRIBUTIONS E.K. designed and performed the experiments, analyzed the data and wrote the paper. J.B. designed and performed the experiments, analyzed the data and wrote the paper. E.R. supervised the project, designed the experiments and wrote the paper.

COMPETING FINANCIAL INTERESTS The authors declare no competing financial interests.

Published online at http://www.natureprotocols.com/.
Reprints and permissions information is available online at http://www.nature.com/reprints/index.html.

1. Palmer, A.E., Qin, Y., Park, J.G. & McCombs, J.E. Design and application of genetically encoded biosensors. *Trends Biotechnol.* **29**, 144–152 (2011).
2. Merlot, S. & Firtel, R.A. Leading the way: directional sensing through phosphatidylinositol 3-kinase and other signaling pathways. *J. Cell Sci.* **116**, 3471–3478 (2003).
3. Devreotes, P. & Janetopoulos, C. Eukaryotic chemotaxis: distinctions between directional sensing and polarization. *J. Biol. Chem.* **278**, 20445–20448 (2003).
4. Tsien, R.Y. & Miyawaki, A. Seeing the machinery of live cells. *Science (New York, NY)* **280**, 1954–1955 (1998).
5. Jares-Erijman, E.A. & Jovin, T.M. FRET imaging. *Nat. Biotechnol.* **21**, 1387–1395 (2003).

6. Kiyokawa, E., Hara, S., Nakamura, T. & Matsuda, M. Fluorescence (Forster) resonance energy transfer imaging of oncogene activity in living cells. *Cancer Sci.* **97**, 8–15 (2006).
7. VanEngelenburg, S.B. & Palmer, A.E. Fluorescent biosensors of protein function. *Curr. Opin. Chem. Biol.* **12**, 60–65 (2008).
8. Kraynov, V.S. *et al.* Localized Rac activation dynamics visualized in living cells. *Science (New York, NY)* **290**, 333–337 (2000).
9. Pertz, O., Hodgson, L., Klemke, R.L. & Hahn, K.M. Spatiotemporal dynamics of RhoA activity in migrating cells. *Nature* **440**, 1069–1072 (2006).
10. Gaits, F. & Hahn, K. Shedding light on cell signaling: interpretation of FRET biosensors. *Sci. STKE* **2003**, PE3 (2003).
11. Aoki, K. & Matsuda, M. Visualization of small GTPase activity with fluorescence resonance energy transfer-based biosensors. *Nat. Protoc.* **4**, 1623–1631 (2009).
12. Esposito, A., Gralle, M., Dani, M.A., Lange, D. & Wouters, F.S. pHlameleons: a family of FRET-based protein sensors for quantitative pH imaging. *Biochemistry* **47**, 13115–13126 (2008).
13. Miyawaki, A. *et al.* Fluorescent indicators for Ca2+ based on green fluorescent proteins and calmodulin. *Nature* **388**, 882–887 (1997).
14. Palmer, A.E. & Tsien, R.Y. Measuring calcium signaling using genetically targetable fluorescent indicators. *Nat. Protoc.* **1**, 1057–1065 (2006).
15. Itoh, R.E. *et al.* Activation of rac and cdc42 video imaged by fluorescent resonance energy transfer-based single-molecule probes in the membrane of living cells. *Mol. Cell Biol.* **22**, 6582–6591 (2002).
16. Wang, Y. *et al.* Visualizing the mechanical activation of Src. *Nature* **434**, 1040–1045 (2005).
17. Fosbrink, M., Aye-Han, N.N., Cheong, R., Levchenko, A. & Zhang, J. Visualization of JNK activity dynamics with a genetically encoded fluorescent biosensor. *Proc. Natl. Acad. Sci. USA* **107**, 5459–5464 (2010).
18. Sato, M., Kawai, Y. & Umezawa, Y. Genetically encoded fluorescent indicators to visualize protein phosphorylation by extracellular signal-regulated kinase in single living cells. *Anal. Chem.* **79**, 2570–2575 (2007).
19. Kiyokawa, E., Aoki, K., Nakamura, T. & Matsuda, M. Spatiotemporal regulation of small GTPases as revealed by probes based on the principle of Forster Resonance Energy Transfer (FRET): implications for signaling and pharmacology. *Ann. Rev. Pharmacol. Toxicol.* **51**, 337–358 (2011).
20. Kardash, E. *et al.* A role for Rho GTPases and cell-cell adhesion in single-cell motility *in vivo*. *Nat. Cell Biol.* **12**, 47–53; sup pp 1–11 (2010).
21. Miyagi, C. *et al.* STAT3 noncell-autonomously controls planar cell polarity during zebrafish convergence and extension. *J. Cell Biol.* **166**, 975–981 (2004).
22. Stockholm, D. *et al.* Imaging calpain protease activity by multiphoton FRET in living mice. *J. Mol. Biol.* **346**, 215–222 (2005).
23. Blaser, H. *et al.* Migration of zebrafish primordial germ cells: a role for Myosin contraction and cytoplasmic flow. *Dev. Cell* **11**, 613–627 (2006).
24. Kamiyama, D. & Chiba, A. Endogenous activation patterns of Cdc42 GTPase within Drosophila embryos. *Science (New York, NY)* **324**, 1338–1340 (2009).
25. Wang, X., He, L., Wu, Y.I., Hahn, K.M. & Montell, D.J. Light-mediated activation reveals a key role for Rac in collective guidance of cell movement *in vivo*. *Nat. Cell Biol.* **12**, 591–597 (2010).
26. Horikawa, K. *et al.* Spontaneous network activity visualized by ultrasensitive Ca(2+) indicators, yellow Cameleon-Nano. *Nat. Methods* **7**, 729–732 (2010).
27. Xia, Z. & Liu, Y. Reliable and global measurement of fluorescence resonance energy transfer using fluorescence microscopes. *Biophys. J.* **81**, 2395–2402 (2001).
28. Nakamura, T., Aoki, K. & Matsuda, M. Monitoring spatio-temporal regulation of Ras and Rho GTPase with GFP-based FRET probes. *Methods* **37**, 146–153 (2005).
29. Köprunner, M., Thisse, C., Thisse, B. & Raz, E. A zebrafish nanos-related gene is essential for the development of primordial germ cells. *Genes Dev.* **15**, 2877–2885 (2001).
30. Goedhart, J. & Kremers, G.-J. in *Laboratory Techniques in Biochemistry and Molecular Biology, FRET and FLIM Techniques*, Vol. 33 (ed. Gadella, T.W.) Ch. 5, 171–223 (Elsevier, 2009).
31. Nguyen, A.W. & Daugherty, P.S. Evolutionary optimization of fluorescent proteins for intracellular FRET. *Nat. Biotechnol.* **23**, 355–360 (2005).
32. Shaner, N.C., Steinbach, P.A. & Tsien, R.Y. A guide to choosing fluorescent proteins. *Nat. Methods* **2**, 905–909 (2005).
33. Ouyang, M., Sun, J., Chien, S. & Wang, Y. Determination of hierarchical relationship of Src and Rac at subcellular locations with FRET biosensors. *Proc. Natl. Acad. Sci. USA* **105**, 14353–14358 (2008).
34. Diekmann, D. *et al.* Bcr encodes a GTPase-activating protein for p21rac. *Nature* **351**, 400–402 (1991).
35. Westerfield, M. *The Zebrafish Book. A Guide for the Laboratory Use of zebrafish (Danio rerio)*, 4th edn. (University of Oregon Press, 2000).
36. Rosen, J.N., Sweeney, M.F. & Mably, J.D. Microinjection of zebrafish embryos to analyze gene function. *J. Vis. Exp.* published online, doi:10.3791/1115 (9 March 2009).
37. Griesbeck, O., Baird, G.S., Campbell, R.E., Zacharias, D.A. & Tsien, R.Y. Reducing the environmental sensitivity of yellow fluorescent protein. Mechanism and applications. *J. Biol. Chem.* **276**, 29188–29194 (2001).